Supplementary Material

Theoretical investigation of high-pressure phase stability and potential superconductivity of Ce-S-H ternary hydrides

Yin L. Xu[1,2], Yang M. Chen[1,*], Xiao Z. Yan[1,*] and Hua Y. Geng[2,3,*]

[1] *School of Science, Key Laboratory of Low Dimensional Quantum Materials and Sensor Devices of Jiangxi Education Institutes, Jiangxi University of Science and Technology, Ganzhou 341000, Jiangxi, P. R. China;*

[2] *National Key Laboratory of Shock Wave and Detonation Physics, Institute of Fluid Physics, China Academy of Engineering Physics, Mianyang, Sichuan 621900, P. R. China;*

[3] *HEDPS, Center for Applied Physics and Technology, and College of Engineering, Peking University, Beijing 100871, P. R. China;*

* *Corresponding authors. E-mail: chenyangmei@jxust.edu.cn; yanxiaozhen@jxust.edu.cn*; *s102genghy@caep.cn*;

TABLE S1. The k-point grid and energy cutoff convergence tests for *Cm*-$CeSH_9$ at 150 GPa.

K-mesh	Energy (eV)	Delta H (eV/atom)	ENCUT	Energy (eV)	Delta H (eV/atom)
1 × 1 × 1	-14.533415		300	8.6711936	
2 × 2 × 2	8.0274123	2.0509843	350	8.4847013	-0.0169538
3 × 3 × 3	8.4033805	0.0341789	400	8.3630379	-0.0110603
4 × 4 × 4	8.2103657	-0.0175468	450	8.2894166	-0.0066928
5 × 5 × 5	8.1988732	-0.0010447	500	8.2510538	-0.0034875
6 × 6 × 6	8.1823005	-0.0015066	550	8.2287587	-0.0020268
7 × 7 × 7	8.2075138	0.0022921	600	8.2123979	-0.0014873
8 × 8 × 8	8.2042772	-0.0002942	650	8.2042773	-0.0007382
9 × 9 × 9	8.2017175	-0.0002327	700	8.1991067	-0.0004700

TABLE S2. The k-point grid and energy cutoff convergence tests for *Cc*-$CeSH_{10}$ at

K-mesh	Energy (eV)	Delta H (eV/atom)	ENCUT	Energy (eV)	Delta H (eV/atom)
1 × 1 × 1	62.667469		300	86.16229	
2 × 2 × 2	84.568892	0.912559284	350	85.64011	-0.021757658
3 × 3 × 3	84.698439	0.005397798	400	85.36256	-0.011564397
4 × 4 × 4	84.871649	0.007217085	450	85.19970	-0.006785838
5 × 5 × 5	84.932403	0.002531437	500	85.10074	-0.004123174
6 × 6 × 6	84.950244	0.000743378	550	85.04224	-0.002437818
7 × 7 × 7	84.955117	0.000203032	600	84.99694	-0.001887214
8 × 8 × 8	84.960385	0.000219503	650	84.96736	-0.001232748
9 × 9 × 9	84.961280	0.000037269	700	84.94813	-0.000801234

300 GPa.

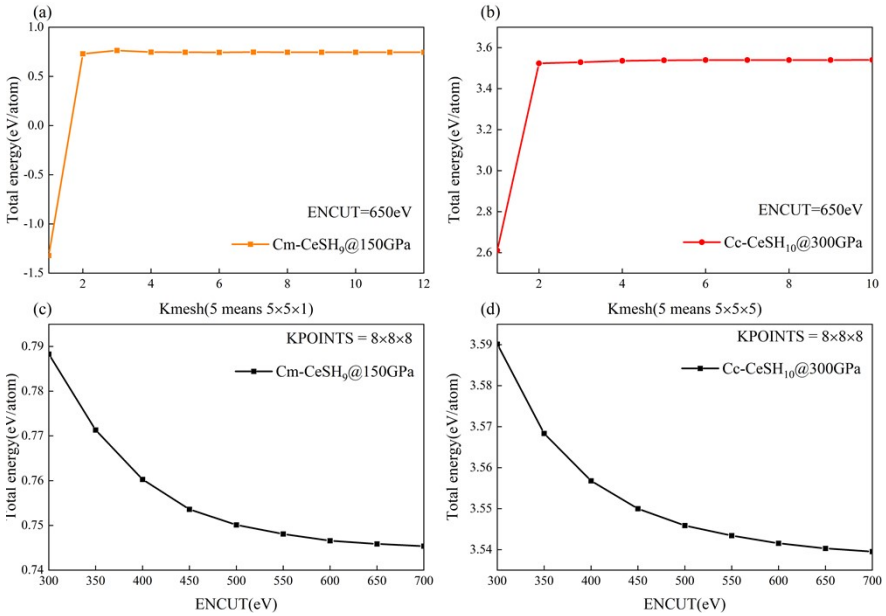

Fig. S1 The total energy convergence tests of *Cm*-$CeSH_9$ (150 GPa) and *Cc*-$CeSH_{10}$ (300 GPa).

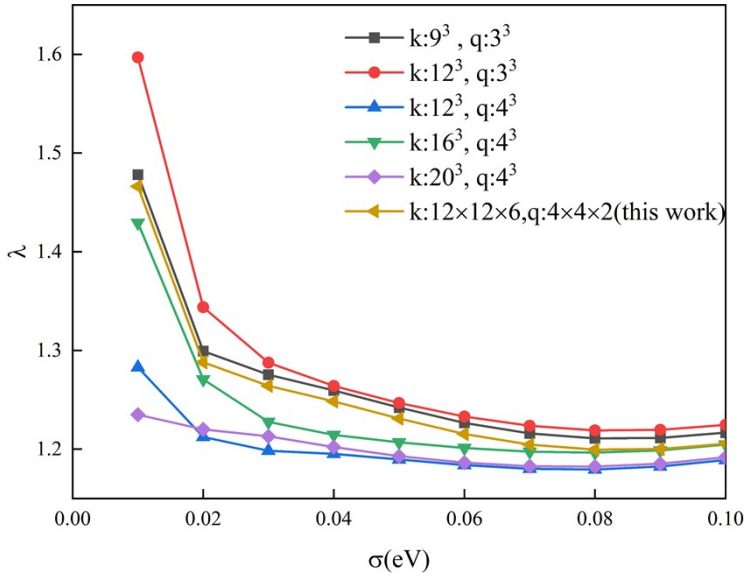

Fig. S2 The k- and q-point mesh tests of *Cm*-$CeSH_9$ (150 GPa).

TABLE S3. The k and q-point mesh for EPC calculations tests of *Cm*-$CeSH_9$ at 150 GPa (degauss =0.08).

K-q mesh	ω_{log} **(K)**	λ	T_c **(K)** (μ^***=0.10)**
k:9^3, q:3^3	818.778	1.21084	74.115
k:12^3, q:3^3	801.19	1.21899	73.116
k:12^3, q:4^3	830.984	1.17944	72.813
k:16^3, q:4^3	820.559	1.19650	73.198
k:20^3, q:4^3	830.161	1.18227	72.961

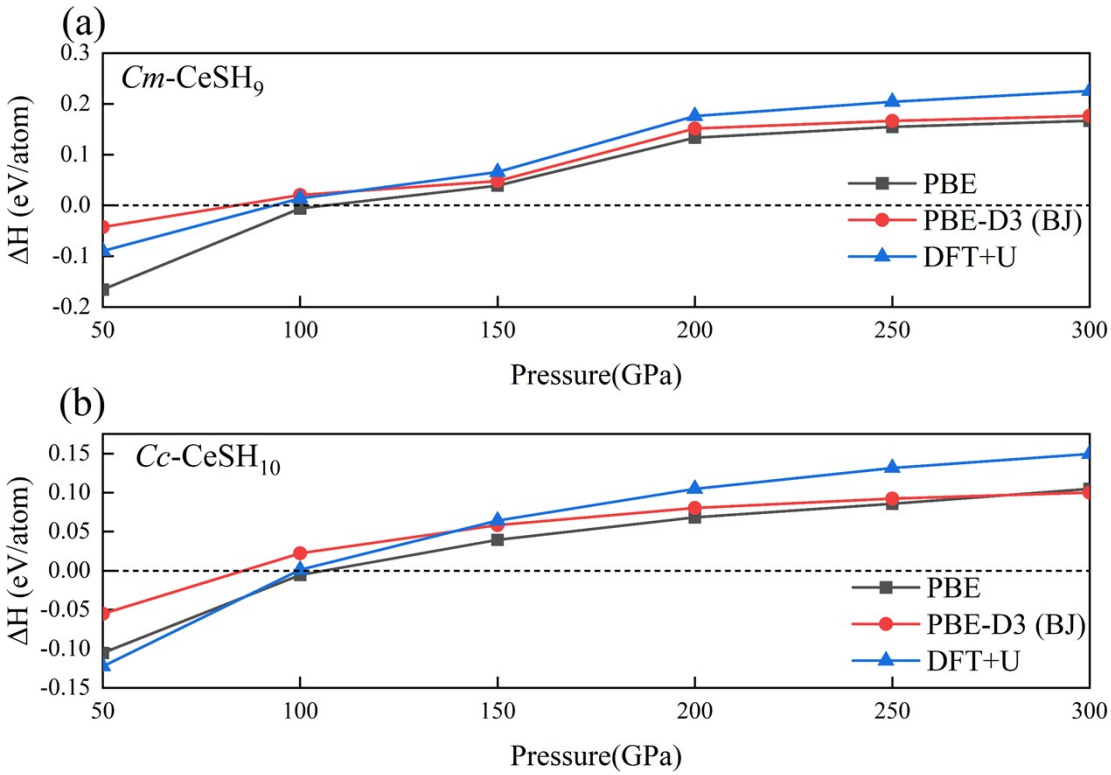

Fig. S3 Comparison of enthalpy difference calculated by different functional approaches for (a) *Cm*-$CeSH_9$ and (b) *Cc*-$CeSH_{10}$.

To evaluate the effect of vdW corrections, we applied the PBE-D3(BJ) method to two representative structures, *Cm*-$CeSH_9$ at 150 GPa and *Cc*-$CeSH_{10}$ at 300 GPa. As shown in **Fig. R3**, including vdW corrections leads to an energy difference of 0.07–0.1 eV/atom for both structures in the 50–300 GPa range. At 50 GPa, the energy variation increases to ~0.1 eV/atom for *Cm*-$CeSH_9$ and ~0.05 eV/atom for *Cc*-$CeSH_{10}$, due to larger interatomic separations enhancing weak long-range interactions. Although vdW corrections affect the calculated formation enthalpy, they do not significantly alter the thermodynamically stable pressure range (where formation enthalpy is negative), shifting it by only ~18 GPa.

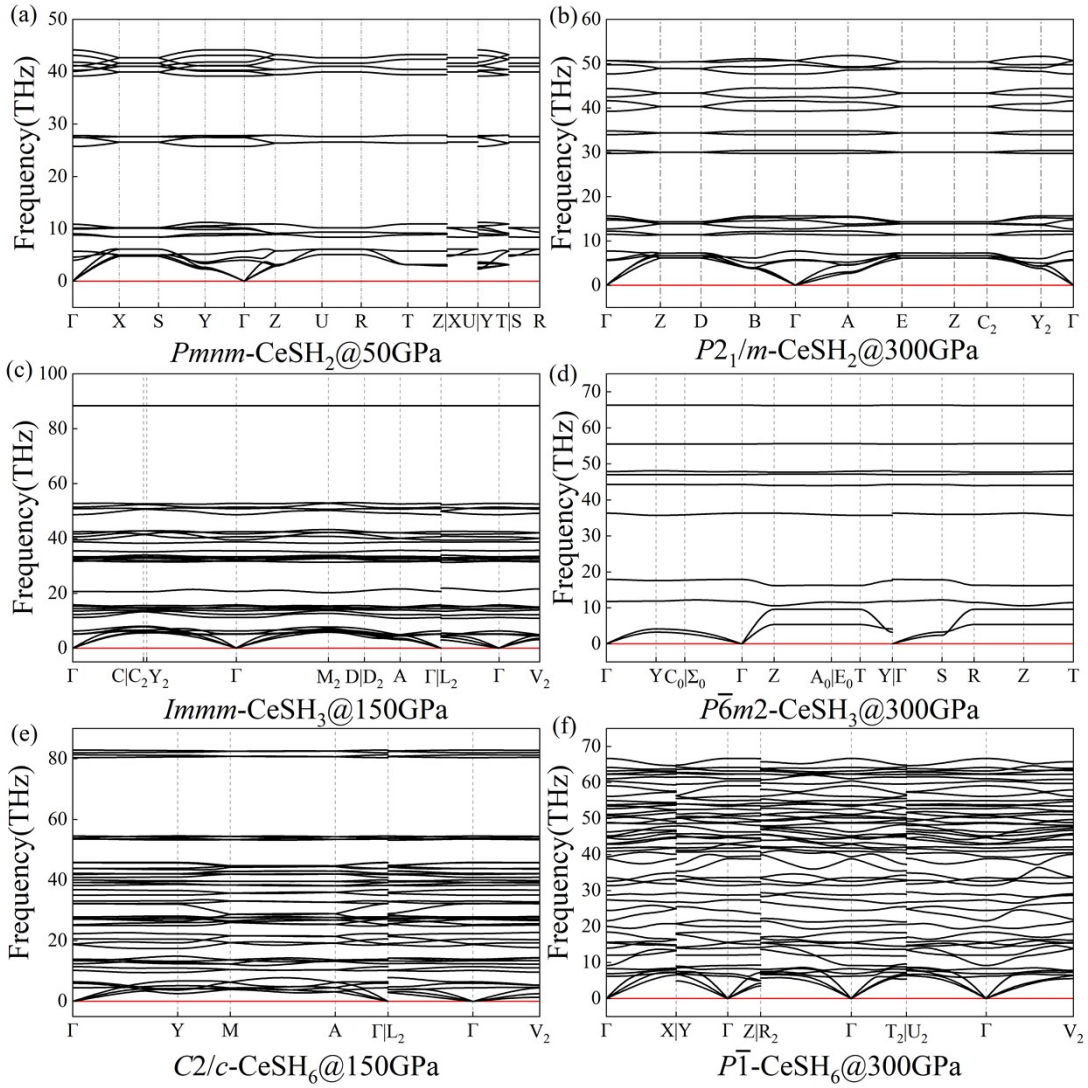

Fig. S4 Phonon dispersion curves. (a) *Pmnm*-$CeSH_2$ (50 GPa), (b) $P2_1/m$-$CeSH_2$ (300 GPa), (c) *Immm*-$CeSH_3$ (150 GPa), (d) $P\bar{6}m2$-$CeSH_3$ (300 GPa), (e) $C2/c$-$CeSH_6$ (150 GPa) and (f) $P\bar{1}$-$CeSH_6$ (300 GPa).

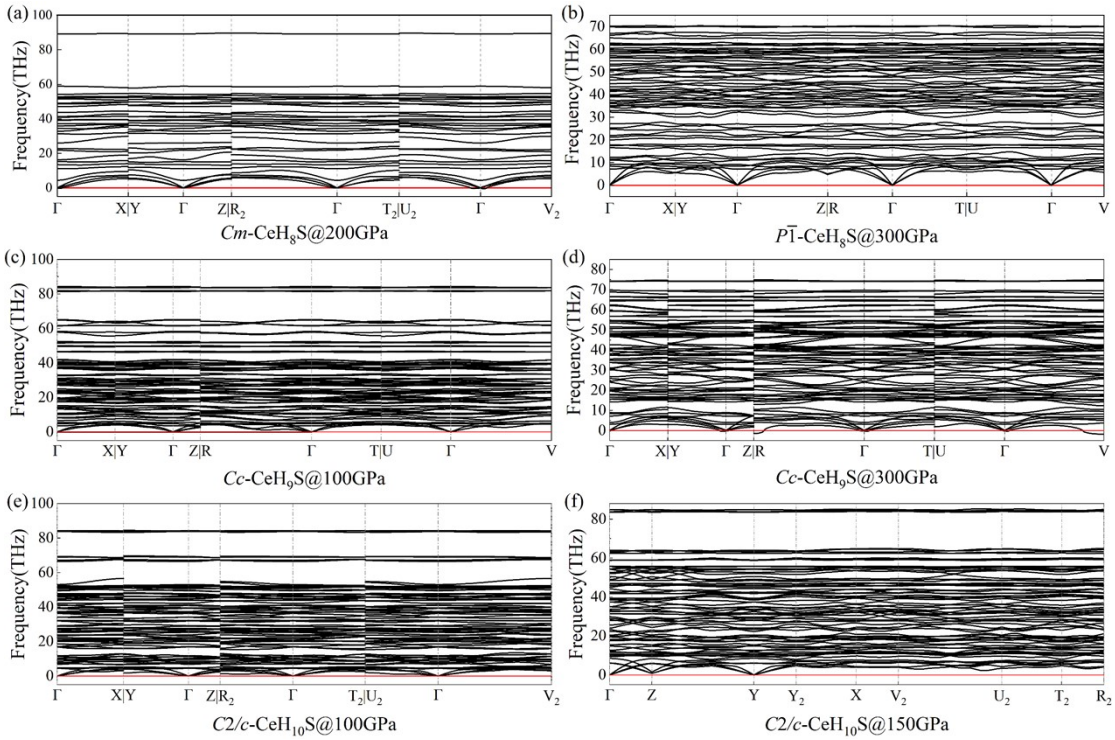

Fig. S5 Phonon dispersion curves. (a) *Cm*-$CeSH_8$ (200 GPa), (b) $P\bar{1}$-$CeSH_8$ (300 GPa), (c) *Cc*-$CeSH_9$ (100 GPa), (d) *Cc*-$CeSH_9$ (300 GPa), (e) $C2/c$-$CeSH_{10}$ (100 GPa) and (f) $C2/c$-$CeSH_{10}$ (150 GPa).

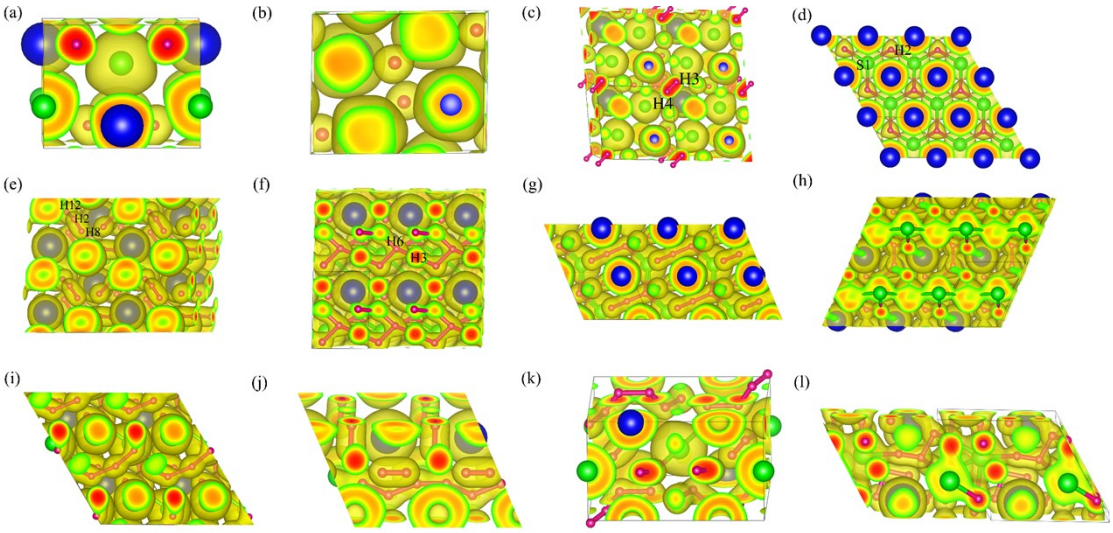

Fig. S6 Electron localization function. (a) *Pmnm*-$CeSH_2$ (50 GPa), (b) $P2_1/m$-$CeSH_2$ (300 GPa), (c) *Immm*-$CeSH_3$ (150 GPa), (d) $P\bar{6}m2$-$CeSH_3$ (300 GPa), (e) $C2/c$-$CeSH_6$ (150 GPa), (f) $P\bar{1}$-$CeSH_6$ (300 GPa), (g) *Cm*-$CeSH_8$ (200 GPa), (h) $P\bar{1}$-$CeSH_8$ (300 GPa), (i) *Cc*-$CeSH_9$ (100 GPa), (j) *Cm*-$CeSH_9$ (150 GPa), (k) $C2/c$-$CeSH_{10}$ (150 GPa) and (l) *Cc*-$CeSH_{10}$ (300 GPa).

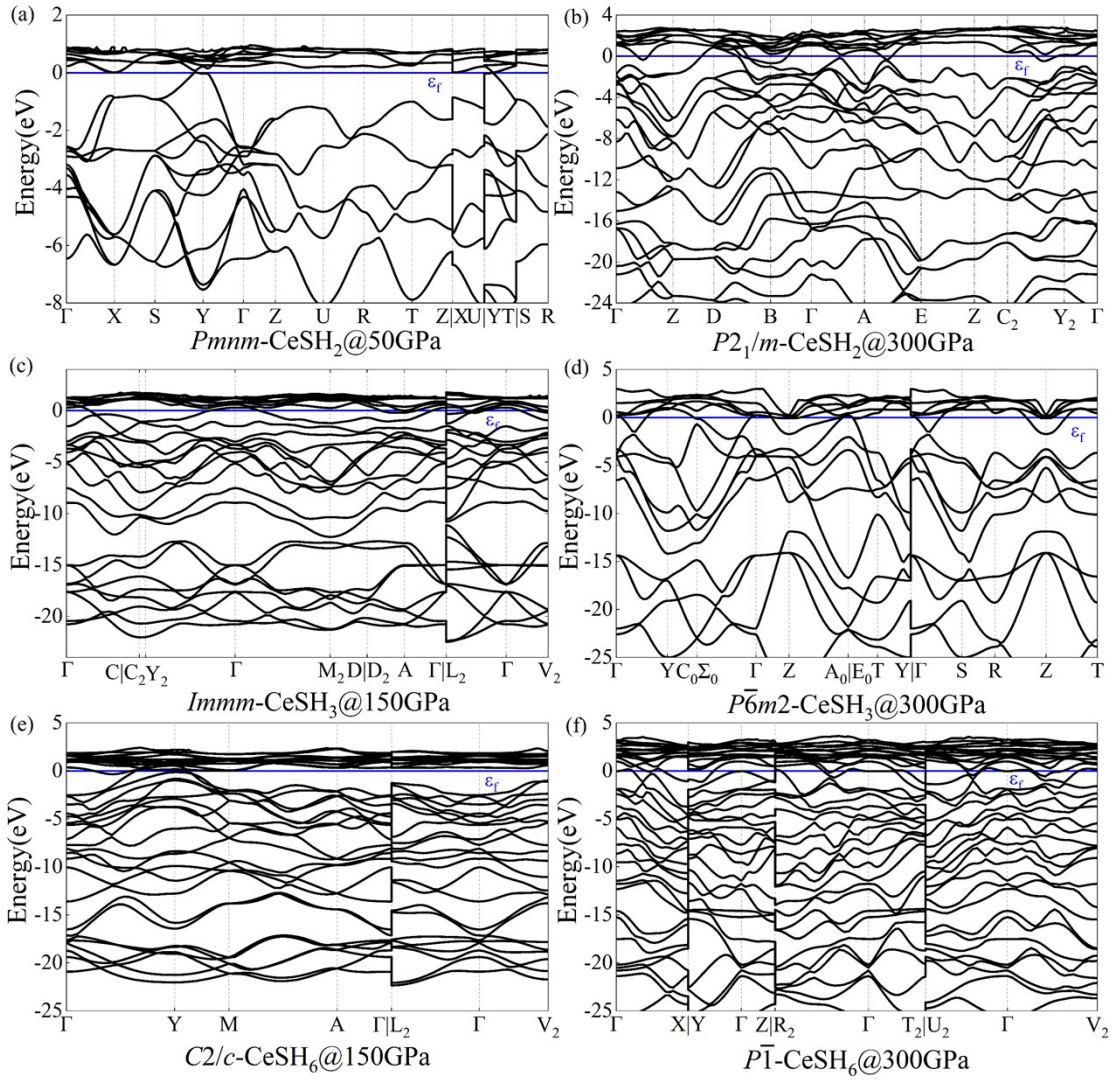

Fig. S7 Electronic band structures. (a) *Pmnm*-$CeSH_2$ (50 GPa), (b) $P2_1/m$-$CeSH_2$ (300 GPa), (c) *Immm*-$CeSH_3$ (150 GPa), (d) $P\bar{6}m2$-$CeSH_3$ (300 GPa), (e) $C2/c$-$CeSH_6$ (150 GPa) and (f) $P\bar{1}$-$CeSH_6$ (300 GPa).

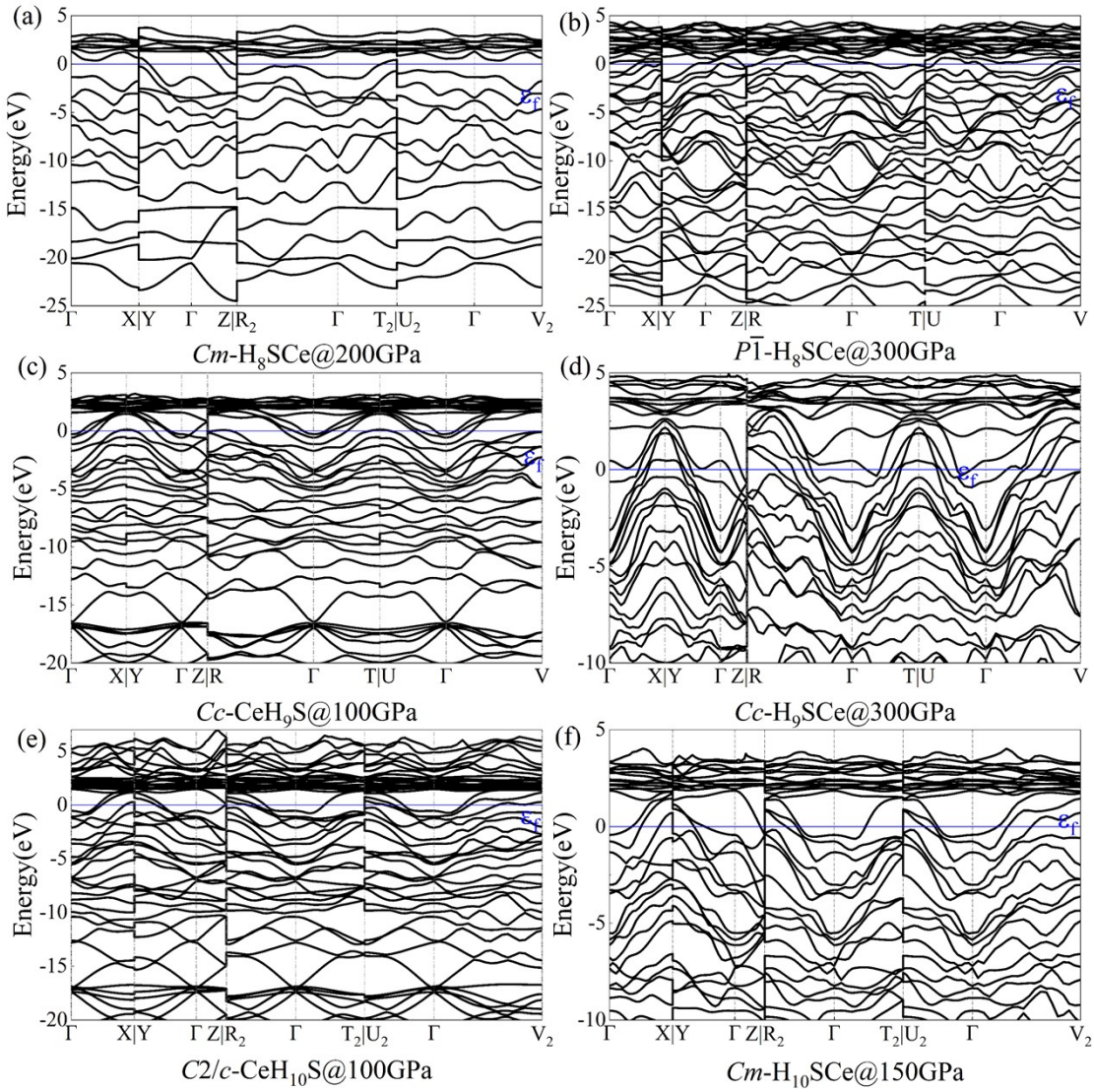

Fig. S8 Electronic band structures. (a) *Cm*-$CeSH_8$ (200 GPa), (b) $P\bar{1}$-$CeSH_8$ (300 GPa), (c) *Cc*-$CeSH_9$ (100 GPa), (d) *Cc*-$CeSH_9$ (300 GPa), (e) $C2/c$-$CeSH_{10}$ (100 GPa) and (f) $C2/c$-$CeSH_{10}$ (150 GPa).

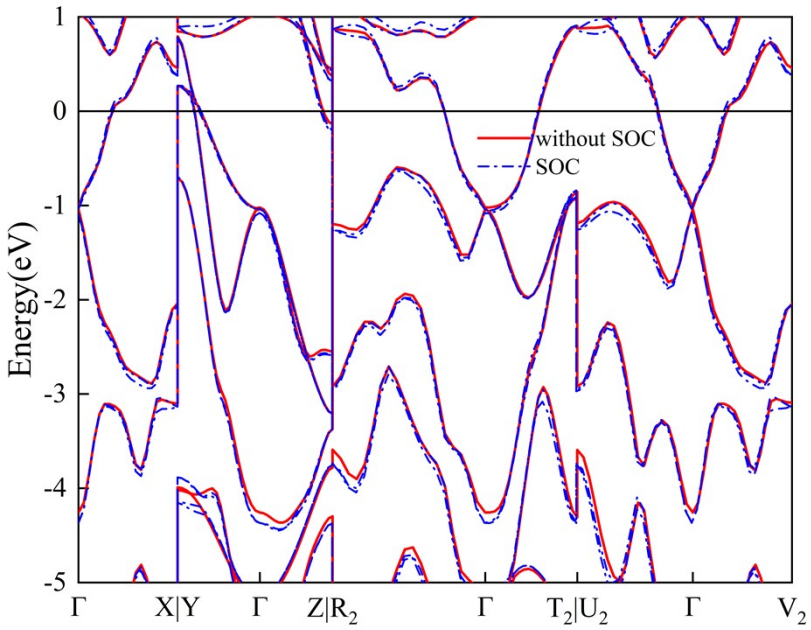

Fig. S9 Comparison of band structure for *Cm*-$CeSH_9$ at 150 GPa. The blue line represents the SOC calculation and the red line represents the calculation without SOC.

We have performed self-consistent electronic structure calculations including spin-orbit coupling (SOC) for the *Cm*-$CeSH_9$ phase. As shown in Fig. R4, the inclusion of SOC leaves the overall band structure largely unchanged. The Fermi energy shifts slightly from 14.496 eV to 14.566 eV (a difference of ~0.07 eV). These subtle modifications originate from the fine adjustments to localized electronic states induced by SOC, which has a negligible influence on the λ and ω_{log}. As a result, SOC primarily leads to a slight splitting of the band structures, while the overall Fermi surface and band topology remain almost unchanged. This demonstrates that SOC has only a minor influence on the electronic structure and thus on the superconducting properties of the system. Given its minimal effect combined with the substantial computational cost, SOC was not included in the remaining calculations.

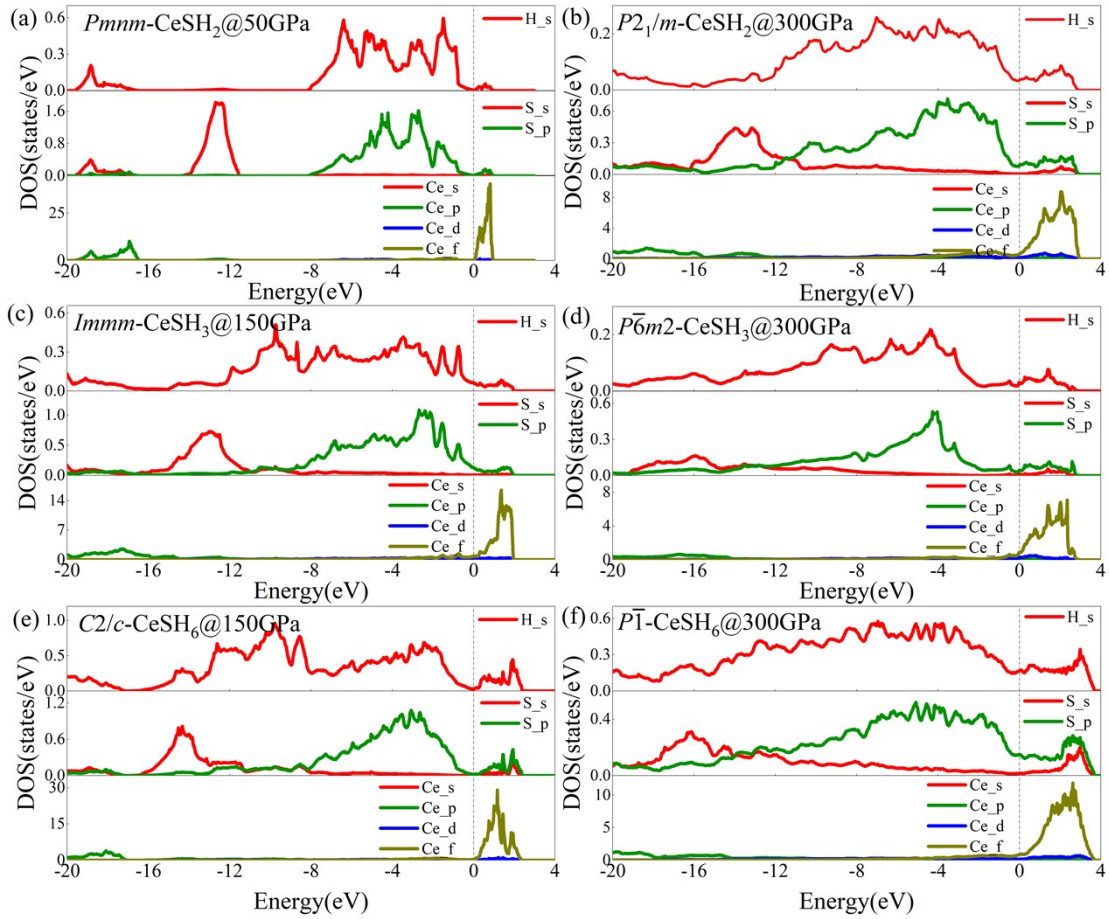

Fig. S10 Partial density of states. (a) *Pmnm*-$CeSH_2$ (50 GPa), (b) $P2_1/m$-$CeSH_2$ (300 GPa), (c) *Immm*-$CeSH_3$ (150 GPa), (d) $P\bar{6}m2$-$CeSH_3$ (300 GPa), (e) $C2/c$-$CeSH_6$ (150 GPa) and (f) $P\bar{1}$-$CeSH_6$ (300 GPa).

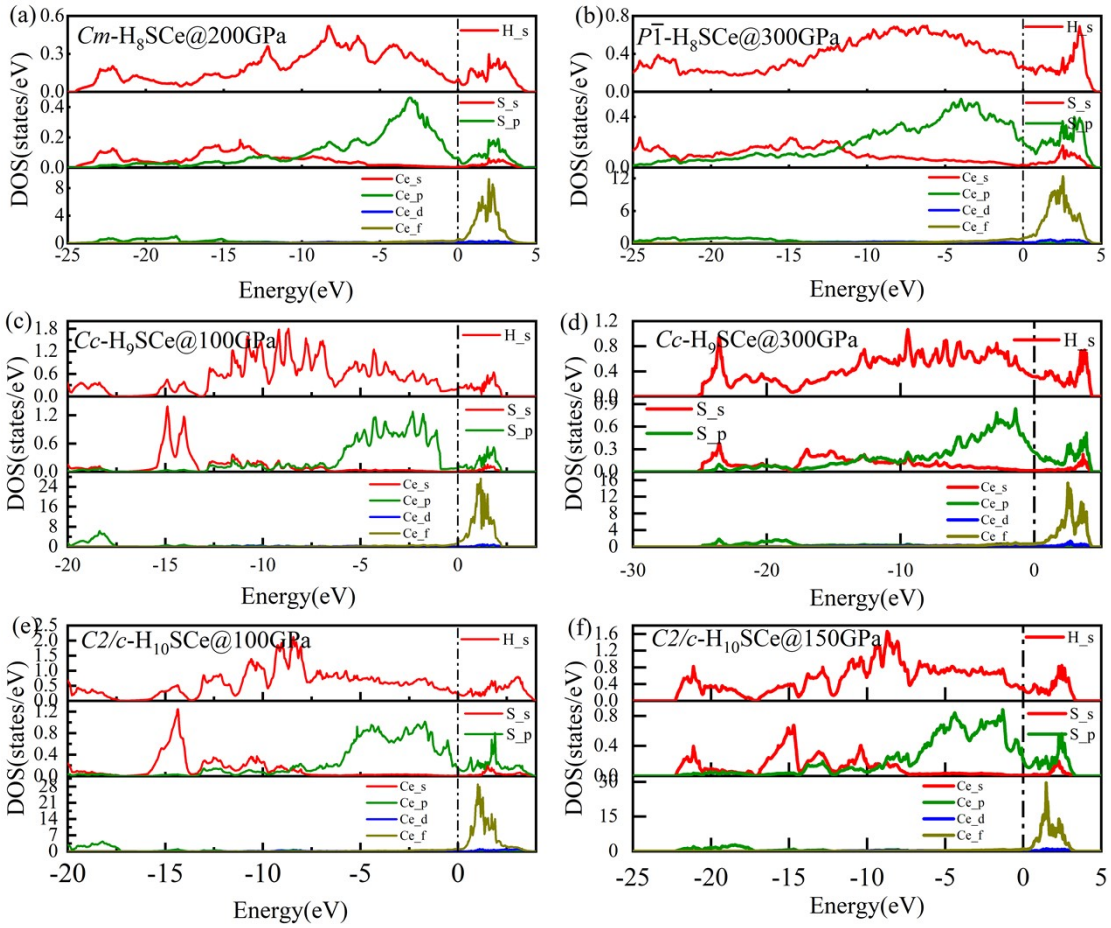

Fig. S11 Partial density of states. (a) *Cm*-$CeSH_8$ (200 GPa), (b) $P\bar{1}$-$CeSH_8$ (300 GPa), (c) *Cc*-$CeSH_9$ (100 GPa), (d) *Cc*-$CeSH_9$ (300 GPa), (e) $C2/c$-$CeSH_{10}$ (100 GPa) and (f) $C2/c$-$CeSH_{10}$ (150 GPa).

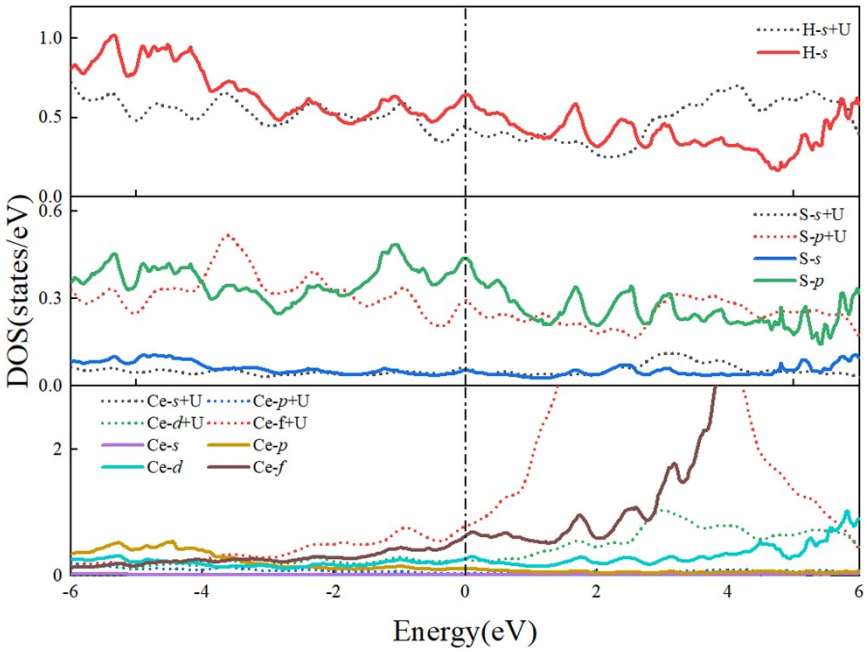

Fig. S12 Comparison of partial density of states for *Cc*-$CeSH_{10}$ at 300 GPa using DFT+U and without U.

We have performed DFT+U calculations with U_{eff}=4 eV on both *Cm*-$CeSH_9$ and *Cc*-$CeSH_{10}$. As shown in Figs. R3 and R5, the inclusion of the +U correction leads to energy difference in the formation enthalpy of 0.05 eV/atom for *Cm*-$CeSH_9$ and 0.04 eV/atom for *Cc*-$CeSH_{10}$ under high pressure. These differences do not significantly affect the stable pressure range, merely shifting the critical pressure at which the formation enthalpy becomes negative by approximately 13 GPa. In the electronic density of states (Fig. S12), the DFT+U method reduces the projected DOS values of the H-s and S-p orbitals, while increasing the projected DOS value of the Ce-f orbital at the Fermi level. Therefore, the DFT+U correction may have a considerable impact on the predicted electron-phonon coupling λ and Tc. However, in the Quantum ESPRESSO package, the DFT+U method is currently not technically feasible for calculating electron-phonon coupling, so we cannot further investigate superconductivity with +U corrections. Nevertheless, we believe that our results are at least qualitatively reliable, and DFT+U calculations may introduce some corrections to the electron-phonon coupling parameter and superconducting transition temperature. In addition, the selection of U values itself involves inherent uncertainty.

TABLE S4. The comparison of enthalpy difference and crystal parameter for *Cm*-

$CeSH_9$ and *Cc*-$CeSH_{10}$ using different method and pseudopotential.

Phase	Pressure (GPa)	Method	Pseudopotential	Enthalpy difference (eV/f.u.)	a (Å)	b (Å)	c (Å)
Cm-$CeSH_9$	150	VASP	PAW	0.04792	3.0354	3.8053	3.9428
Cm-$CeSH_9$	150	QE	USPP	0.02899	3.0381	3.8040	3.3945
Cc-$CeSH_{10}$	300	VASP	PAW	0.10008	3.3787	4.662	4.8240
Cc-$CeSH_{10}$	300	QE	USPP	0.04916	3.3660	4.6876	4.8238

Table S5 Lattice parameters and atomic positions for predicted Ce-H-S systems

Compound	Pressure (GPa)	Space group	Lattice parameters (Å, degree)	Atomic positions			
$CeSH_2$	50	*Pmnm*	a=3.466	H1	0.000	0.843	0.210
			b=4.111	H2	0.500	0.157	0.710
			c=5.224	H3	0.000	0.843	0.790
			α=β=γ=90	H4	0.500	0.157	0.290
				S1	0.000	0.338	0.000
				S2	0.500	0.662	0.500
				Ce1	0.000	0.182	0.500
				Ce2	0.500	0.818	0.000
$CeSH_2$	300	$P2_1/m$	a=3.687	H1	0.477	0.250	0.645
			b=c=3.703	H2	0.051	0.750	0.129
			α=102.95	H3	0.523	0.750	0.355
			β=γ=104.28	H4	0.949	0.250	0.874
				S1	0.670	0.750	0.859
				S2	0.330	0.250	0.140
				Ce1	0.190	0.750	0.653
				Ce2	0.810	0.250	0.347
$CeSH_3$	150	*Immm*	a=2.826	H1	0.167	0.035	0.374
			b=c=4.771	H2	0.830	0.374	0.035
			α=95.83	H3	0.000	0.065	0.065
			β=107.23	H4	0.000	0.935	0.935
			γ=72.77	H5	0.830	0.965	0.626
				H6	0.170	0.626	0.965
				S1	0.500	0.698	0.698
				S2	0.500	0.301	0.301
				Ce1	0.252	0.248	0.752
				Ce2	0.748	0.752	0.248
$CeSH_3$	300	$P\bar{6}m2$	a=b=2.725	H1	0.000	0.000	0.500
			c=3.641	H2	0.333	0.667	0.705
			α=β=90	H3	0.333	0.667	0.295
			γ=120	S1	0.667	0.333	0.500
				Ce1	0.000	0.000	0.000
$CeSH_6$	50	$Cmc2_1$	a=3.671	H1	0.023	0.384	0.910
			b=4.870	H2	0.751	0.499	0.710
			c=5.622	H3	0.549	0.135	0.969
			α=β=90	H4	0.684	0.865	0.469
			γ=67.85	H5	0.249	0.501	0.210

				H6	0.737	0.526	0.559
				H7	0.263	0.474	0.059
				H8	0.592	0.384	0.910
				H9	0.316	0.135	0.969
				H10	0.977	0.616	0.410
				H11	0.408	0.616	0.410
				H12	0.451	0.865	0.469
				S1	0.932	0.136	0.268
				S2	0.068	0.864	0.768
				Ce1	0.355	0.291	0.612
				Ce2	0.645	0.709	0.112
$CeSH_6$	150	C^2/c	a=b=3.872	H1	0.491	0.235	0.363
			c=4.780	H2	0.691	0.773	0.534
			α=β=89.80	H3	0.773	0.691	0.034
			γ=103.40	H4	0.429	0.210	0.096
				H5	0.765	0.509	0.137
				H6	0.227	0.309	0.966
				H7	0.571	0.790	0.904
				H8	0.509	0.765	0.637
				H9	0.235	0.491	0.863
				H10	0.210	0.429	0.596
				H11	0.309	0.227	0.466
				H12	0.790	0.571	0.403
				S1	0.888	0.112	0.250
				S2	0.112	0.888	0.750
				Ce1	0.709	0.291	0.750
				Ce2	0.291	0.709	0.250
$CeSH_6$	300	$P\bar{1}$	a=2.662	H1	0.243	0.635	0.521
			b=3.671	H2	0.757	0.365	0.479
			c=5.772	H3	0.845	0.189	0.968
			α=101.62	H4	0.186	0.479	0.939
			β=85.27	H5	0.735	0.209	0.736
			γ=90.26	H6	0.469	0.292	0.911
				H7	0.814	0.521	0.061
				H8	0.265	0.791	0.264
				H9	0.531	0.708	0.089
				H10	0.823	0.927	0.099
				H11	0.157	0.811	0.032
				H12	0.177	0.073	0.901
				S1	0.234	0.178	0.611
				S2	0.766	0.822	0.389
				Ce1	0.298	0.282	0.226

				Ce2	0.702	0.718	0.774
$CeSH_8$	200	*Cm*	a=2.743	H1	0.545	0.088	0.411
			b=3.662	H2	0.656	0.311	0.164
			c=3.900	H3	0.382	0.764	0.383
			α=105.10	H4	0.769	0.539	0.507
			β=90.01	H5	0.433	0.867	0.708
			γ=112.00	H6	0.896	0.790	0.533
				H7	0.591	0.182	0.853
				H8	0.244	0.488	0.227
				S1	0.158	0.316	0.658
				Ce1	0.927	0.854	0.050
$CeSH_8$	300	$P\bar{1}$	a=3.475	H1	0.641	0.748	0.798
			b=4.544	H2	0.612	0.293	0.698
			c=4.682	H3	0.382	0.230	0.493
			α=115.28	H4	0.777	0.128	0.716
			β=96.99	H5	0.115	0.252	0.057
			γ=107.73	H6	0.359	0.252	0.202
				H7	0.171	0.498	0.336
				H8	0.223	0.872	0.284
				H9	0.326	0.489	0.514
				H10	0.388	0.707	0.302
				H11	0.885	0.748	0.943
				H12	0.674	0.511	0.486
				H13	0.788	0.055	0.891
				H14	0.618	0.770	0.507
				H15	0.829	0.502	0.664
				H16	0.212	0.945	0.109
				S1	0.243	0.509	0.877
				S2	0.757	0.491	0.123
				Ce1	0.203	0.919	0.698
				Ce2	0.797	0.081	0.302

$CeSH_9$	150	*Cm*	a=3.028	H1	0.568	0.137	0.490
			b=3.800	H2	0.476	0.952	0.744
			c=3.934	H3	0.345	0.690	0.719
			α=105.89	H4	0.964	0.280	0.557
			β=90.00	H5	0.346	0.692	0.045
			γ=113.48	H6	0.480	0.961	0.152
				H7	0.604	0.498	0.832
				H8	0.316	0.280	0.557
				H9	0.894	0.498	0.832
				S1	0.072	0.144	0.005
				Ce1	0.842	0.685	0.377
$CeSH_9$	300	*Cc*	a=3.372	H1	0.020	0.951	0.369
			b=3.372	H2	0.951	0.020	0.869
			c=6.470	H3	0.814	0.065	0.297
			α=98.61	H4	0.065	0.814	0.797
			β=98.61	H5	0.382	0.791	0.679
			γ=115.11	H6	0.791	0.382	0.179
				H7	0.412	0.161	0.491
				H8	0.752	0.535	0.619
				H9	0.896	0.646	0.459
				H10	0.161	0.412	0.991
				H11	0.535	0.752	0.119
				H12	0.646	0.896	0.959
				H13	0.250	0.681	0.870
				H14	0.201	0.916	0.619
				H15	0.630	0.719	0.679
				H16	0.681	0.250	0.370
				H17	0.916	0.201	0.119
				H18	0.719	0.630	0.179
				S1	0.226	0.976	0.120
				S2	0.976	0.226	0.620
				Ce1	0.606	0.356	0.880
				Ce2	0.356	0.606	0.380

$CeSH_{10}$	150	C^2/c	a=3.718	H1	0.450	0.086	0.163
			b=3.790	H2	0.462	0.086	0.336
			c=6.82	H3	0.549	0.913	0.836
			α=90.93	H4	0.537	0.913	0.663
			β=91.90	H5	0.623	0.862	0.419
			γ=60.62	H6	0.514	0.862	0.080
				H7	0.376	0.137	0.580
				H8	0.485	0.137	0.919
				H9	0.895	0.536	0.302
				H10	0.297	0.838	0.001
				H11	0.443	0.442	0.125
				H12	0.568	0.536	0.197
				H13	0.863	0.838	0.498
				H14	0.114	0.442	0.374
				H15	0.104	0.463	0.697
				H16	0.702	0.161	0.998
				H17	0.556	0.557	0.874
				H18	0.431	0.463	0.802
				H19	0.136	0.161	0.501
				H20	0.885	0.557	0.625
				S1	0.000	0.500	0.000
				S2	0.500	0.500	0.500
				Ce1	0.007	0.985	0.250
				Ce2	0.992	0.014	0.750
$CeSH_{10}$	300	*Cc*	a=3.361	H1	0.556	0.148	0.316
			b=4.683	H2	0.243	0.397	0.707
			c=4.830	H3	0.986	0.765	0.717
			α=60.95	H4	0.771	0.831	0.104
			β=88.29	H5	0.259	0.140	0.900
			γ=90.12	H6	0.506	0.486	0.290
				H7	0.255	0.934	0.897
				H8	0.757	0.052	0.118
				H9	0.708	0.366	0.197
				H10	0.269	0.100	0.508
				H11	0.763	0.592	0.322
				H12	0.007	0.490	0.748
				H13	0.746	0.621	0.498
				H14	0.235	0.886	0.692
				H15	0.764	0.953	0.415
				H16	0.994	0.212	0.009
				H17	0.001	0.741	0.998
				H18	0.268	0.355	0.532
				H19	0.516	0.203	0.022

H20	0.513	0.762	0.009
S1	0.574	0.587	0.814
S2	0.123	0.398	0.169
Ce1	0.254	0.817	0.331
Ce2	0.761	0.153	0.675

Table S6 Bader charge analysis of $P\bar{6}m2$-CeH_3S at 300 GPa.

Atom	Charge value/e	Charge transfer $\sigma(e)$
H1	1.026541	0.026541
H2	1.131832	0.131832
H3	1.132118	0.132118
S1	6.487279	0.487279
Ce	11.222231	-0.777769

Table S7 Bader charge analysis of $P\bar{1}$-CeH_6S at 300 GPa·

Atom	Charge value/e	Charge transfer $\sigma(e)$
H1	1.100623	0.100623
H2	1.100625	0.100625
H3	1.091454	0.091454
H4	1.113393	0.113393
H5	1.000168	0.000168
H6	1.054464	0.054464
H7	1.115207	0.115207
H8	1.000168	0.000168
H9	1.054342	0.054342
H10	1.126221	0.126221
H11	1.091454	0.091454
H12	1.126087	0.126087
S1	6.371285	0.371285
S2	6.372501	0.372501
Ce1	11.141046	-0.858954
Ce2	11.140960	-0.85904

Table S8 Bader charge analysis of *Cm*-CeH_8S at 200 GPa·

Atom	Charge value/e	Charge transfer $\sigma(e)$
H1	1.0767	0.0767
H2	1.2005	0.2005
H3	1.0380	0.0380
H4	0.9146	-0.0854
H5	1.1482	0.1482
H6	1.1063	0.1063
H7	0.9563	-0.0437
H8	1.1321	0.1321
S1	6.5747	0.5747
Ce1	10.8527	-1.1473